Fabrication, Estimation and Trypsin Digestion Experiment of the Thermally Isolated Micro Teactor for Bio-chemical Reaction

Tae Seok Sim, Dae Weon Kim, Eun-Mi Kim, Hwang Soo Joo, Kook-Nyung Lee, Byung Gee Kim, Yong Hyup Kim, and Yong-Kweon Kim

Abstract—**This paper describes design, fabrication, and application of the silicon based temperature controllable micro reactor. In order to achieve fast temperature variation and low energy consumption, reaction chamber of the micro reactor was thermally isolated by etching the highly conductive silicon around the reaction chamber. Compared with the model not having thermally isolated structure, the thermally isolated micro reactor showed enhanced thermal performances such as fast temperature variation and low energy consumption. The performance enhancements of the micro reactor due to etched holes were verified by thermal experiment and numerical analysis. Regarding to 42 percents reduction of the thermal mass achieved by the etched holes, approximately 4 times faster thermal variation and 5 times smaller energy consumption were acquired. The total size of the fabricated micro reactor was 37×30×1 mm^3. Microchannel and reaction chamber were formed on the silicon substrate. The openings of channel and chamber were covered by the glass substrate. The Pt electrodes for heater and sensor are fabricated on the backside of silicon substrate below the reaction chamber. The dimension of channel cross section was 200×100 μm^2. The volume of reaction chamber was 4 μl. The temperature of the micro reactor was controlled and measured simultaneously with NI DAQ PCI-MIO-16E-1 board and LabVIEW program. Finally, the fabricated micro reactor and the temperature control system were applied to the thermal denaturation and the trypsin digestion of protein. BSA (bovine serum albumin) was chosen for the test sample. It was successfully shown that BSA was successfully denatured at 75°C for 1 min and digested by trypsin at 37°C for 10 min.**

Index Terms—**BioMEMS, microreactor, temperature control, thermal isolation, thermal denaturation, trypsin digestion**

I. INTRODUCTION

MEMS techniques are increasingly used in various fields of bio-chemistry to realize more efficient structures than conventional macroscopic systems. In addition to generally used chemical and biological analysis applications, microfabricated reactors have a number of advantages in the application of bio-chemical reaction, chemical kinetics studies, and process development. The small quantity of chemicals prevents experimental accidents such as explosion and leakage of the toxic gas. Because of their small size, microreactors provide high area to volume ratios, high heat and mass transfer rates. Moreover, microreactors can be integrated with sensors and other process unit operations, including temperature sensors, cooling channels, and detection system, creating capabilities exceeding those of conventional macroscale units. New reaction method not achieved with conventional reactors, e.g., direct fluorination of aromatic compounds could be possible. The direct fluorination of aromatic compounds is highly exothermic and thus very difficult to control on a large scale. Poor solublility of fluorine results in reactions that proceed at the liquid-gas

Manuscript received December 19, 2004; revised August 10, 2005.
School of Electrical Engineering and Computer Science, Seoul National University, Seoul, Korea.
e-mail: sim93@snu.ac.kr

interface. Consequently, localized hot spots are likely to form in large-scale systems, which can lead to unwanted side reaction. Among the several advantages in microfluidic systems, high heat and mass transfer rates allow reactions to be performed under more accurate and higher yield condition than can be achieved with conventional macroscopic reactors [1, 2]. PCR (polymerase chain reaction) chip is a typical application to the bio-chemical reaction [3-9]. Fuel cell is another example of the micro reactor applied to the chemical kinetics. As a demonstration of process development, DuPont has synthesized a number of potentially hazardous chemicals, including isocyanates in 1996 [10]. In this paper, we proposed and fabricated a thermally isolated temperature controllable micro reactor having several etched holes to enhance the thermal performances such as fast thermal variation and low energy consumption. To evaluate the effect of etched holes numerically and experimentally, we fabricated a micro reactor not having etched holes and compared the acquired numerical and experimental results each other. Finally, among several applications of micro reactor, the fabricated micro reactor was applied to the thermal denaturation and the trypsin digestion, which are the common bio-chemical reactions related to the proteins. For the convenience of the explanation, the micro reactor having several etched holes will be called as a thermal isolation model and the micro reactor not having etched holes as a normal model.

II. Design, Fabrication and Implementation

Fig. 1 shows schematic views of the thermal isolation model whose reaction chamber is thermally isolated by several etched holes and the normal model which does not have any etched holes. Micro channel and reaction chamber are formed on the silicon substrate, and the open side is covered by glass substrate. Pt heater and sensor are fabricated on the bottom of the silicon substrate below the reaction chamber. Since the heat conductivity of glass is much smaller than that of silicon ($k_{silicon}$=148, k_{glass}=1.4 W/m·K), the glass substrate acts as a thermal insulator. The total dimension of the micro reactor is 37×30×1 mm^3 and the dimension of channel cross section is 200×100 μm^2. Reaction chamber is designed to have elliptical shape to minimize dead volume. The volume of the reaction chamber is 4 μl. Fig. 2 shows the mask layout of the Pt electrodes. The heater is located below the reaction chamber with the similar shape of the reaction chamber to minimize the undesirable thermal dissipation from the heater to the silicon substrate. We choose the thickness of Pt electrodes as 1000 Å. The width of heater electrode is 200 μm and the width of sensor electrode is 50 μm, respectively. The resistance of Pt heater and sensor at 20 °C can be determined by the following equation (1) [11].

$$R= \frac{\rho L}{A} \tag{1}$$

In the above equation (1), ρ represents resistivity (Ω·m) of Pt, L is the length (m) of the Pt electrode and A is the cross-section area (m^2) of the Pt electrode. The resistivity of the sputtered Pt is generally varied by sputtering environment. In this case, the acquired resistivity of Pt thin film is approximately 18×10^{-8} Ω·m at 20 °C. The designed resistance of sensor is 1898 Ω and the acquired resistance of the fabricated sensor is 1829 Ω (at 20 °C), respectively. The difference between design value and acquired value results from the increase of the dimension of Pt electrodes due to the fabrication errors.

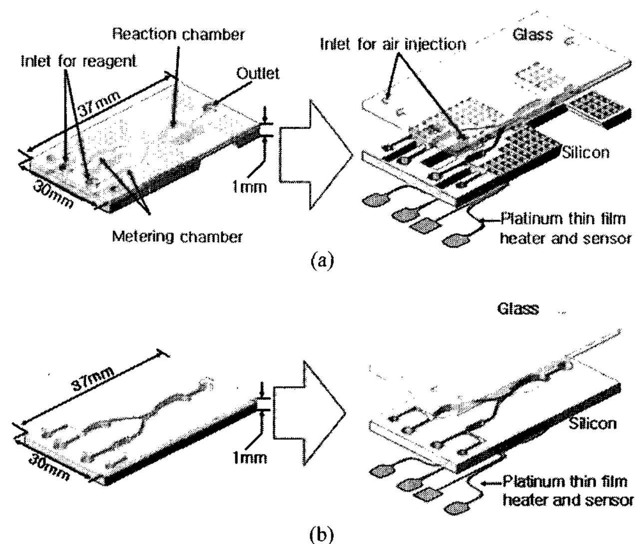

Fig. 1. Schematic view of the fabricated temperature controllable micro reactor, (a) thermal isolation model, (b) normal model.

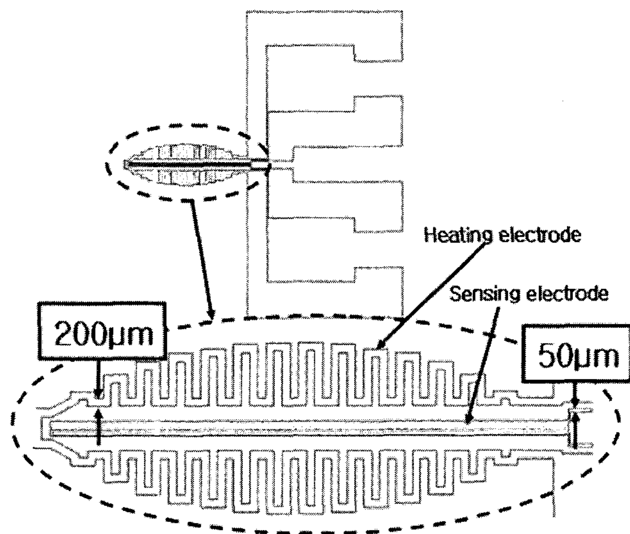

Fig. 2. Layout of the Pt heater and sensor electrodes.

Fig. 3 shows fabrication process of the thermally isolated temperature controllable micro reactor. The used wafer is a double-side polished silicon (100) substrate with a diameter of 100 mm and a thickness of about 500 μm. At first, Si_3N_4 is deposited using LPCVD to the thickness of 1000 Å. The Si_3N_4 layer is patterned by photolithography and etched down to the silicon by reactive ion etching (RIE). And then the silicon substrate was etched to a depth of 100 μm by deep reactive ion etching (DRIE) to form reaction chamber and micro channel. To pattern holes to be etched on the other side of silicon substrate, the above processes such as photolithography and RIE are repeated. Si_3N_4 layer on the top of the silicon substrate is etched away to reveal silicon surface.

The silicon substrate is cleaned with the H_2SO_4 to remove small organic particles completely before anodic bonding. A glass substrate with a thickness of 500 μm was cleaned with H_2SO_4 and laminated by a BF410 film photoresist. The BF410 photoresist was patterned by photolithography to form inlet and outlet holes, and the glass substrate was sandblasted. After alignment, the sandblasted glass substrate was anodically bonded with the previously fabricated silicon substrate. The back side of silicon substrate is etched away using KOH wet etchant (30 wt%, 80 °C, 6.5 hours) to form etched holes. Then the heater and sensor patterns are fabricated by lift off process. A Ti film of 200 Å and a Pt film of 1000 Å are deposited on the patterned bottom side of the silicon substrate by dc off-axis magnetron sputtering. Ti thin film is used as an adhesion layer. The completed wafer was diced into

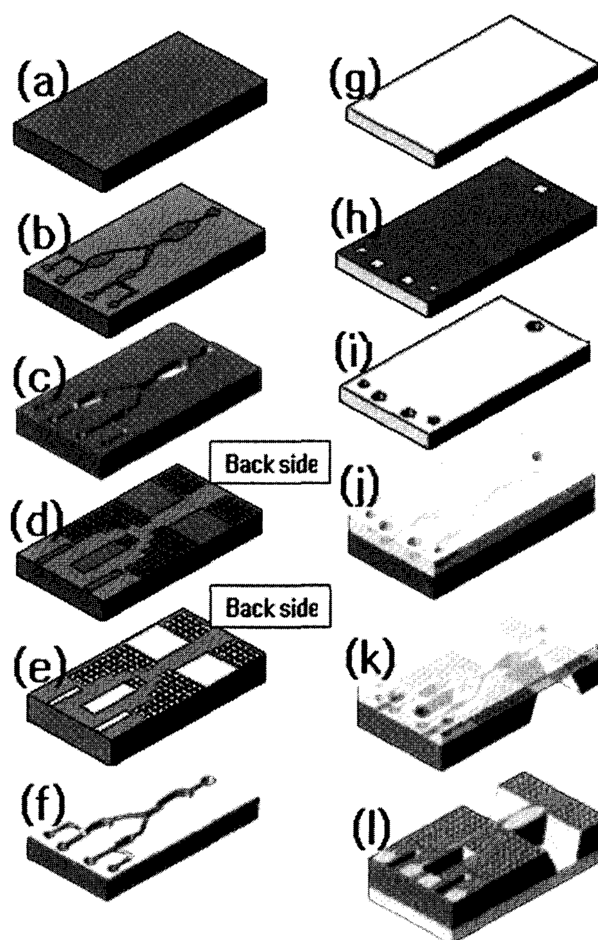

Fig. 3. Process sequences for the fabrication of the thermally isolated temperature controllable micro reactor. (a) 1000 Å LPCVD Si_3N_3, (b) PR patterning, (c) DRIE & PR remove, (d) PR patterning (back side of the silicon), (e) Si_3N_3 patterning & PR remove (back side), (f) Si_3N_3 remove by RIE, (g) glass substrate cleaning with H_2SO_4, (h) BF410 film patterning, (i) sandblasting, (j) anodic bonding, (k) KOH wet etch, (l) Pt patterning by lift-off process (Ti: 200 Å, Pt:1000 Å).

individual temperature controllable micro reactors. The fabricated micro reactors are shown in fig. 4.

To measure and control temperature of the reaction chamber, an external temperature control system is constructed, as shown in fig. 5. Wheatstone bridge is used to transform the resistance variation of the Pt sensor to voltage variation. The measured voltage is amplified by the instrumentation amplifier (AD524) and transferred to the analog input of the data acquisition board (DAQ PCI-MIO-16E-1). The resolution of the DAQ board is 2.4 mV for the range of 0 - 10 V. But the actual voltage range of the Pt sensor is very small compared to the full range of data acquisition board. Therefore it is desirable to amplify the voltage of Pt sensor. The amplification of the measured voltage increases resolution in reading the temperature and

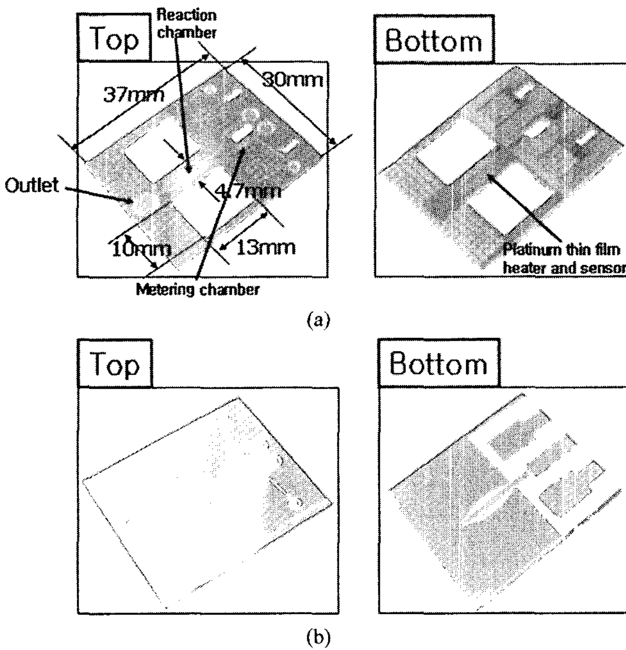

Fig. 4. Photographs of the fabricated micro reactors. (a) thermal isolation model, (b) normal model.

decreases measurement noise due to the low resolution. The operational amplifier (Trek 50/750) gives amplified power to the Pt heater in proportion to the analog output of the data acquisition system. In this case, the programmed PID control algorithm adjusts the analog output to control the temperature as fast as possible.

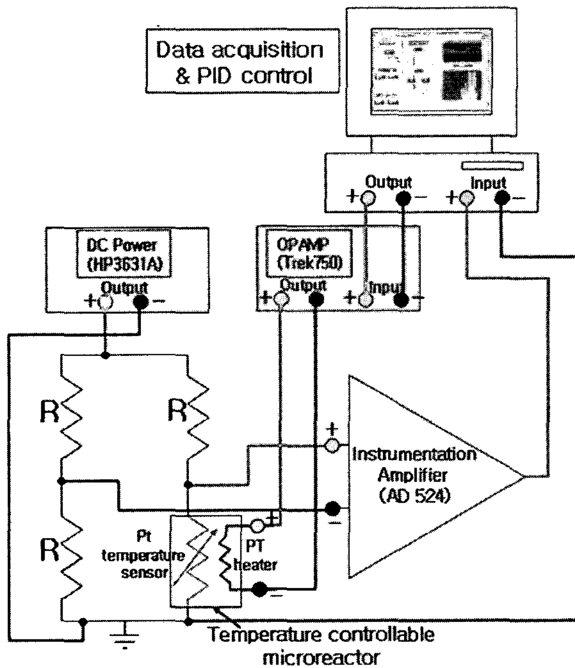

Fig. 5. Schematic diagram for the interface of micro reactor and the external temperature control system.

III. Numerical Analysis

To estimate the effect of the etched holes as a thermal insulator on the thermal dissipation, three dimensional numerical analyses of the proposed thermal isolation model and the normal model were conducted with the ANSYS simulator. The assumptions for the ANSYS simulation are as follows;

(a) Silicon substrate is a homogeneous material.

(b) Air exists with isotropic distribution.

(c) Steady state.

The heat conductivity of the silicon substrate is set to 148 W/m·K and convection coefficient is set to 5 $W/m^2 \cdot K$ as a simulation parameter. Fig. 6 shows the three dimensional steady state heat distributions and the cross-sectional heat distributions of each model. In the three dimensional heat distribution profile (Fig. 6-(a), (b)), it is shown that the reaction chamber of the thermal isolation model is thermally isolated and the heat is condensed to the reaction chamber. Considering the section from b to b′, this inclination is critically shown. The etched holes prevent thermal dissipation through the silicon substrate and increase temperature difference along with the distance from the center as shown in fig. 6-(c), (d).

Fig. 6. The ANSYS simulation results about the heat distribution of the micro reactor. (a) three dimensional heat distribution of the thermal isolation model, (b) three dimensional heat distribution of the normal model, (c) cross-sectional heat distribution of the thermal isolation model, (d). cross-sectional heat distribution of the normal model.

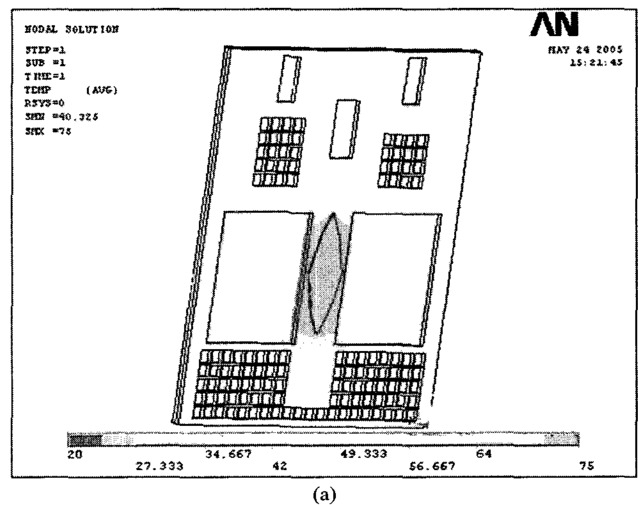

(a)

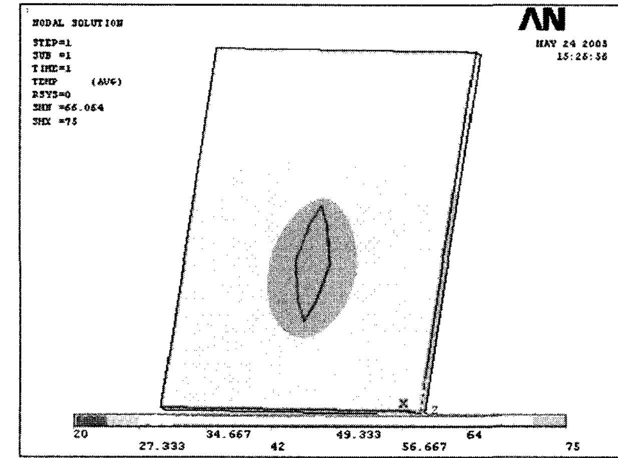

(b)

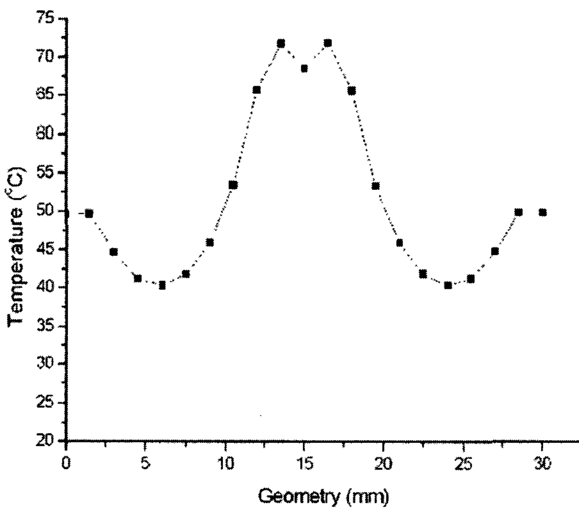

(c)

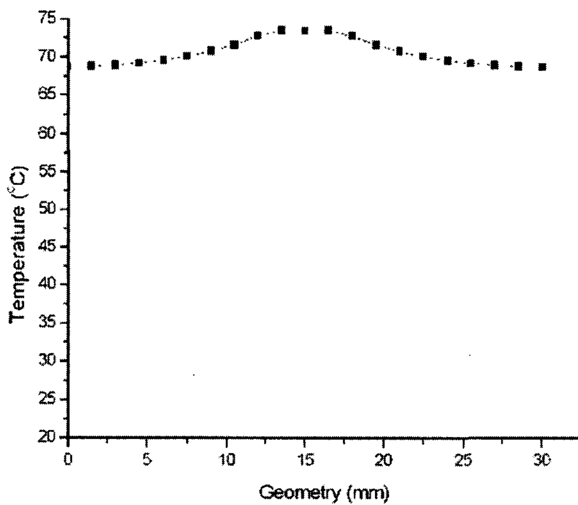

(d)

Fig. 6. The ANSYS simulation results about the heat distribution of the micro reactor. (a) three dimensional heat distribution of the thermal isolation model, (b) three dimensional heat distribution of the normal model, (c) cross-sectional heat distribution of the thermal isolation model, (d). cross-sectional heat distribution of the normal model.

Although the temperature difference between the center and the edge of micro reactor is small, it is successfully shown that the fabricated etched holes still remain as low temperature and block the thermal dissipation from reaction chamber by insulating the thermal conduction through the silicon substrate. From these results, it can be inferred that due to the prevention of the undesirable thermal dissipation by the etched holes, heat can be transferred from Pt heater to the reaction chamber without thermal dissipation in the transient state.

IV. EXPRIMENTAL RESULTS AND DISCUSSIONS

A. Evaluation of the Fabricated Pt sensor

The experiment for the characteristic of the Pt sensor was conducted in an environmental chamber to minimize noises from the air convention and the circumstance condition. The resistance measurement of the Pt sensor with respect to the various temperature is conducted four times, and the results are averaged. The range of temperature for the measurement is from 20 °C to 80 °C, which covers a full range needed to the protein reactions. The temperature range for the protein reactions is typically from 30 to 60 °C. Fig. 7 shows the results of the resistance measurement. The resistance of the Pt sensor shows a good linearity within the measured temperature range with negligible standard deviation (±0.5 Ω). The linear property of the Pt sensor can be expressed by the equation (2) [11, 12],

$$R=R_0\times\left[1+\alpha(T-T_0)\right] \qquad (2)$$

Where R is the resistance of the Pt sensor electrode at temperature T (°C) and α is the TCR (temperature coefficient of resistance) of the Pt thin film. The acquired TCR of the fabricated Pt thin film is 2.02×10^{-3} °C^{-1}.

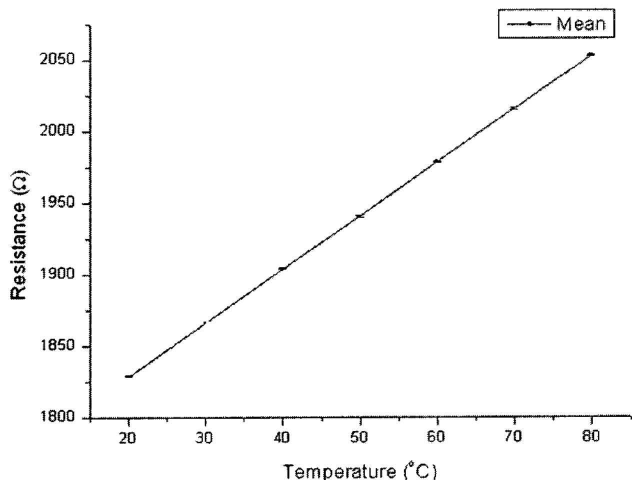

Fig. 7. Statistical plot of sensor resistance with respect to temperature.

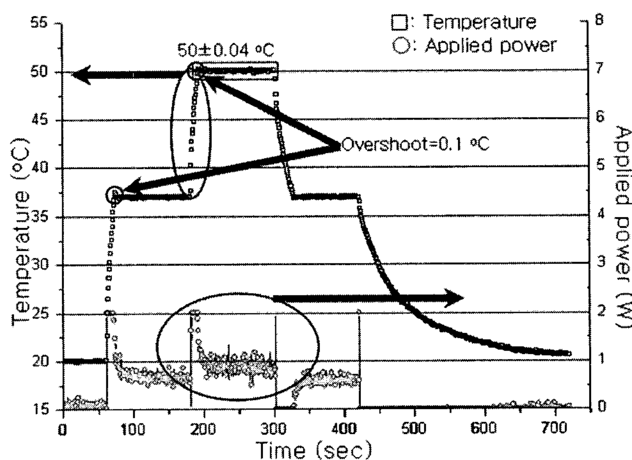

Fig. 8. Plot of the controlled temperature and the applied power.

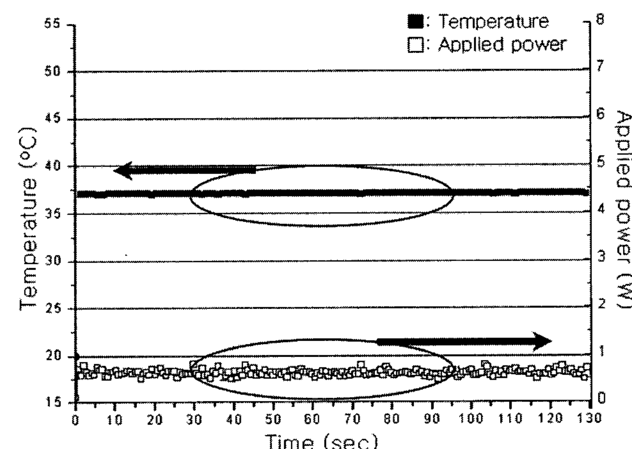

Fig. 9. Plot of the long time temperature control and the applied power.

B. Temperature Control of the Micro Reactor

The evaluation for temperature control system was conducted at the generally used temperatures in protein reaction, e.g., 37 °C and 50 °C. The normal model was used to evaluate temperature control system because the normal model would be the maximum load to the temperature control system. The reaction chamber of the microchip is filled with DI water and heated to 37 °C and 50 °C. As shown in fig. 8, the precise temperature control is achieved with small overshoot (0.1 °C) and steady state error (±0.04 °C). The programmed PID controller successfully adjusts the analog output to control the temperature of reaction chamber. The applied power is set not to exceed 2 W. The heated micro reactor is cooled by natural air convection. Since the PID controller cannot do anything for the rapid cooling, the cooling rate is strictly proportional to the temperature difference with the circumstance. Therefore an external cooling device is needed to acquire the rapid cooling rate regardless to the condition of circumstance.

To confirm the long time stability of the temperature control system, temperature of the micro reactor was controlled for over 130 hours at the fixed temperature of 37 °C. As shown in fig. 9, the temperature is controlled stably for a long time with steady state error less than ± 0.04 °C.

C. Effects of the Etched Holes

To verify the effects of the etched holes, the temperature control experiments using two models were conducted and their results were compared each other. As shown in fig. 10, the thermal isolation model shows more rapid thermal variation as expected. Rising time of the thermal isolation model is approximately 4 times faster than that of the normal model.

The acquired rising times (time from 10 percent to 90 percent of the target temperature) of the thermal isolation model and the normal model are 2.2 sec and 9 sec, respectively. Falling time of the thermal isolation model becomes faster than that of the normal model as well. The amount of the applied energy during the temperature

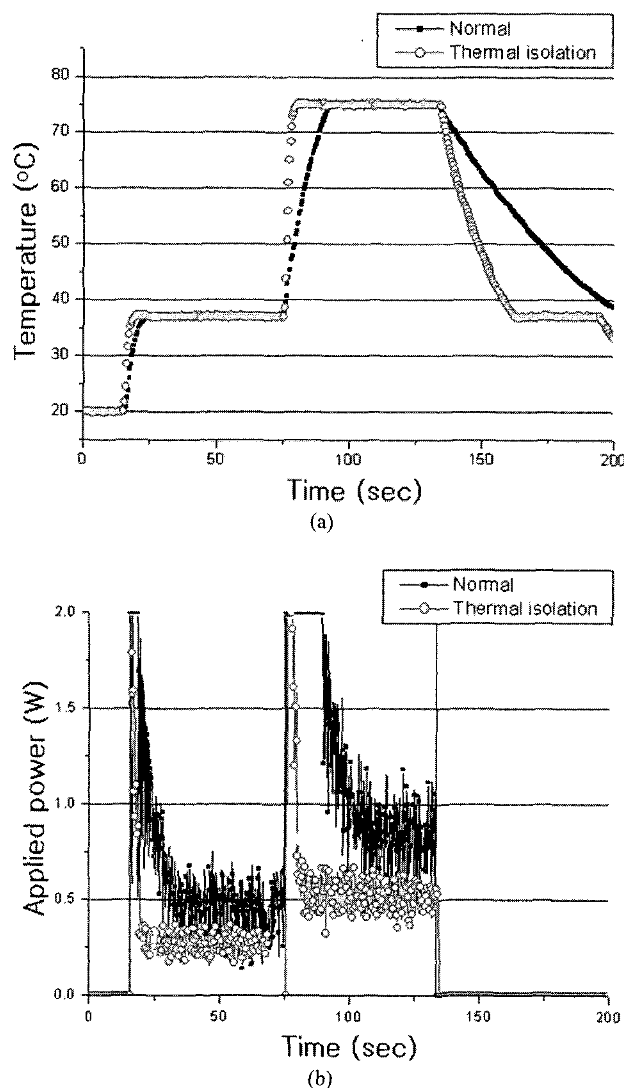

Fig. 10. Plots of temperature control results of the thermal isolation model and the normal model. (a) temperature vs time, (b) applied power vs time.

increase of the reaction chamber is also reduced. The amount of applied energy is calculated by integrating the applied power with respect to the time. As a result of calculation, the consumed energies by the thermal isolation model and the normal model are acquired as 4.06 J and 20.35 J, respectively. The consumed energy of the thermal isolation model is 5 times smaller than that of the normal model. These faster thermal variations and lower energy consumption more than two times assure that the reduction of the thermal mass is not the only factor of the performance enhancement of the micro reactor, because the reduction of thermal mass due to the etched holes is only 42 percent of the normal model. Therefore, from the results of experiment and simulation, it can be inferred that the performance enhancement of the micro reactor is related to both the reduction of thermal mass and the prevention of thermal dissipation by the etched holes.

D. Application

With the instrumented temperature control system, the fabricated micro reactor is applied to the thermal denaturation and typsin digestion. BSA (bovine serum albumin) is chosen for the test sample which is one of the standard proteins for the mass spectrometry. BSA is dissolved in DI (de-ionized) water to make a concentration of 0.2 M. Trypsin is dissolved in aqueous 25 mM ammonium bicarbonate solution (pH 7.8) with a concentration of 4 M. 3 μl of BSA solution is loaded on the outlet of the microreactor with the pipette. And then, the loaded BSA solution is injected into the heat-controllable reaction chamber by capillary force. All the inlets and outlets are sealed with the PDMS cover to prevent evaporation of the BSA solution. After that, thermal denaturation is performed at 75 °C for 1 min. And then, the denatured BSA is exhausted to the outlet and 1 μl of trypsin solution is added and mixed after chilling down to 37°C. The mixture is injected into the reaction chamber again. And BSA is digested by trypsin at 37°C for 10 min. The fluidic control of mixture is achieved by the pressure control using syringe connected to the inlets. The digested BSA was collected with the pipette and analyzed by the MALDI-TOF-MS (matrix assisted laser desorption /ionization time of flight mass spectrometry). As soon as the digestion is completed, all solutions in the chamber are pushed out with syringe. The digested solution is mixed with the same volume of 10 mg/ml -cyano-4-hydroxycinnamic acid (Sigma) in aqueous 70 %(v/v) acetonitrile immediately. The mixed solution is spotted on the MALDI probe. MALDI MS analysis is performed with a Bruker Datonics Biflex IV time of flight mass spectrometry (Bruker, Germany) with delayed extraction condition, operating with a pulsed N_2 laser at 337 nm. Positive ion mass spectra are acquired using reflector mode with an accelerating voltage of 20.0 kV. Each spectrum is the average result of 100 laser shots. Mass calibration was achieved using an external standard. Fig. 11 shows the MALDI-TOF-MS spectrums of the digested BSA. The acquired peak is compared to the standard MS spectrum of

BSA. And then the number of matched peaks to the standard MS spectrum is counted. The thermally denatured BSA shows more matched peptide peaks and the increased intensity (Fig. 11-(b)). The number of acquired matched peaks is 11. The unmatched peaks result from the contamination during experiment. The sequence coverage is about 20 %, which is enough for the MS analysis. This means that the BSA was successfully denatured by the fabricated micro reactor at 75 °C and digested by trypsin at 37 °C with the precise temperature control, because the digestion and the denaturation of BSA are sensitively dependent to the reaction temperature. Unmatched peaks result from the contamination during experiment.

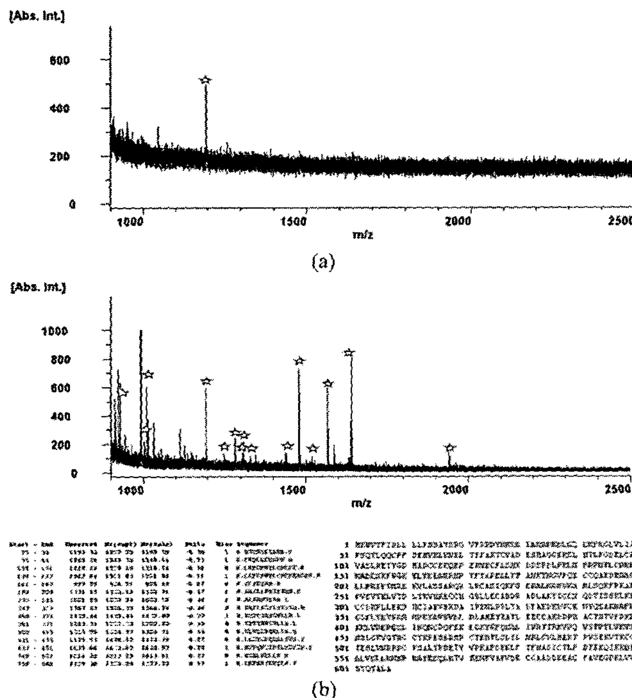

Fig. 11. MALDI-TOF-MS spectrum for the digested BSA. (a) without 75 °C/ 1 min thermal denaturation, (b) with 75 °C/ 1 min thermal denaturation.

V. Conclusions

We have fabricated and estimated the thermally isolated temperature controllable micro reactor and temperature control system. The temperature of the fabricated micro reactor could be controlled by the instrumented temperature control system with small overshoot (0.1 °C) and steady state error (±0.04 °C). The performance enhancement, feasibility and the durability of the fabricated thermally isolated temperature controllable micro reactor and temperature control system were approved by the thermal experiment. It was shown that the heating and cooling rates became faster and the energy consumption became smaller in the thermal isolation model due to the reduction of thermal mass and the prevention of thermal dissipation. The fabricated micro reactor stably operated for more than 130 hours. The result of the numerical analysis showed that the etched holes successfully acted as a thermal insulator to the steady state. As a result, the etched holes played an important role in the thermal insulation and the reduction of thermal mass for the performance enhancement of the micro reactor. The thermal isolation model shows Therefore, it would be the best method to use the etched holes for the performance enhancement of the silicon based temperature controllable micro reactor. Finally, it was shown that the fabricated micro reactor is successfully applied to the bio-chemical reaction with precise temperature control. Protein was successfully denatured and digested by the fabricated micro reactor and temperature control system within 11 minutes.

References

[1] K. F. Jensen, *Chemical Engineering Science*, 56, 293 (2001).

[2] D. S Yoon, Y. S. LEE, H. J. CHO, S. W. SUNG, K. W. OH, J. H. CHA and G. B. Lim, *Journal of Micromechanics and Microengineering*, 12, 813 (2002).

[3] L. J. Kricka, P. Wilding, *Anal Bioanal Chem*, 377, 820 (2003).

[4] J. J. Brandner, G. Emig, M. A. Liauw, K. Schubert, *Chemical Engineering Journal*, 101, 217 (2004).

[5] R. J. Goldstein, E. R. G. Eckert, W. E. Ibele, S. V. Patankar, T. W. Simon, T. H. Kuehn, P. J. Strykowski, K. K. Tamma, J. V. R. Heberlein, J. H. Davidson, J. Bischof, F. A. Kulacki, U. Kortshagen, S. Garrick, *International Journal of Heat an Mass Transfer*, 46, 1887 (2003).

[6] V. Lysenko, S. Périchon, B. Remaki, D. Barbier, *Sensors and Actuators A*, 99, 13 (2002).

[7] Quanbo Zou, Uppili Sridhar, Yu Chen, and Janak Singh, *IEEE Sensors Journal*, 3, 6, 774 (2003).

[8] A. Fuchs, H. Jeanson, P. Claustre, J. A. Gruss, F. Revol-Cavalier, P. Caillat, U. Mastromatteo, M. Scurati, F. Villa, G. Barlocchi, P. Corona, B. Grieco, *2nd Annual International IEEE-EMBS Special Topic Conference on Microtechnologies in Medicine & Biology*, (Wisconsin, USA, May 2-4, 2002), 227.
[9] C. G. J. Schabmueller, M. A. Lee, A. G. R. Evans, A. Brunnschweiler, G. J. Ensell and D. L. Leslie, *Engineering Science and Education Journal*, 275 (2000).
[10] J. J. Lerou, M. P. Harold, J. Ryley, J. Ashmead, T. C. O'Brien, M. Johnson, J. Perrotto, C. T. Blaisdell, T. A. Rensi and J. Nyquist, *Microsystem Technology for Chemical and Biological Micro Reactors*, 132, 51 (1996).
[11] Wilson. A. Clayton, *IEEE Transaction in Industry Applications*, 24, 2, 200 (1988).
[12] Wilson. A. Clayton, Thermoresistive systems in Process Instruments and Controls Handbook, 3rd Edition. (McGraw-Hill, New-York, 1985), 1210.
[13] Z. Y. Park and D. H. Russell, *Analytical Chemistry*, 72, 2667 (2000).

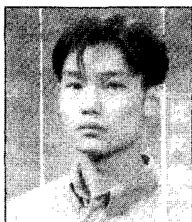

Tae Seok Sim He received the B. S. and M. S. degrees in electrical engineering from Korea University, Seoul, Korea in 1999 and 2001, respectively, and He is currently a Ph.D. candidate at School of Electrical Engineering and Computer Science in Seoul National University, Seoul, Korea. His main recent research activities are micro fluidics and protein chip.

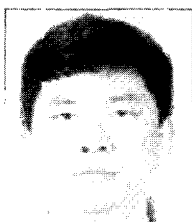

Dae-Weon Kim He received the B.S degree in mechanical engineering from the Pusan National University, Seoul, Korea, in 1990, the M.S degree received with the Computational Fluid Dynamics in 2002 and for Ph. D. course in mechanical and aerospace Engineering of Seoul National University. Also, had been worked at a heavy industrial company of Doosan group for 10 ten years as a engineer of design and overseas team leader in project management.

Eun-Mi Kim She received the B.S. degree in chemical engineering from the Sungkyunkwan University, Seoul, Korea, in 2002, and she is in the M.S. course in Seoul National University. Her current research interests are biochip development and glycosidase screening.

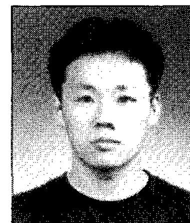

Hwang-Soo Joo He received the B.S. degree in chemical engineering from the Seoul National University, Seoul, Korea, in 2000, and he is in the Ph. D. course in Seoul National University. His current research interests are the study about global regulation of bacteria using proteomics, and the application of biochip and mass spectrometry.

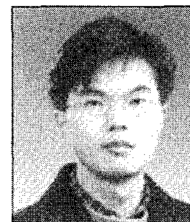

Kook-Nyung Lee He received his B.S., M.S. and Ph.D. degree at the School of Electrical Engineering and Computer Science of Seoul National University in 1998, 2000 and 2003 respectively. His Ph. D dissertation was on Maskless photolithography systems using micromirror array for protein chip fabrication. And now he is doing his post doctoral research at Nano Bioelectronics & Systems Research Center in Seoul National University. Since 1998, he has been working on the design and fabrication of micromirror array for optical modulation, which is used to make surface modification for biochip fabrication. He also worked on the design and fabrication of microwell array with glass bottom for micro ELISA(Enzyme Linked Immuno Sorbent Assay) chip. His current research interests are modeling, design, fabrication and testing of optical MEMS devices and especially bio application of them.

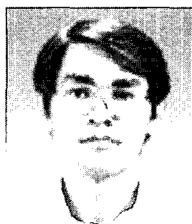

Yong-Hyup Kim He received the B.S. degree in aerospace engineering from the Seoul National University, Seoul, Korea, in 1979, and M.S and the Ph. D. degrees from the University of Maryland, College Park, in 1986 and 1989, respectively. From 1979 to 1995, he joined the Korea Institute of Aeronautical Technology and NASA Langley Research Center. In 1995, he joined the Seoul National University as an assistant professor, where he is currently a professor in school of mechanical and aerospace engineering. His current research interests are nano technology using nanowire and CNT for field emission display, also study of space environment effects.

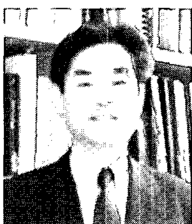

Byung-Gee Kim He received the B.S. and M.S. degrees in chemical engineering from the Seoul National University, Seoul, Korea, in 1980 and 1982, respectively, and the Ph. D. from Cornell University, Ithaca, USA, in 1989. In 1988, he joined the Genencor International Co., USA. In 1991, he joined the Seoul National University as an assistant professor, where he is currently a professor in school of chemical engineering. His current research interests are biocatalysis using cell metabolism and enzymes, cell and genome engineering, proteomics and mass spectrometry.

Yong-Kweon Kim He (S'90-M'90) received the B.S. and M.S. degrees in electrical engineering from the Seoul National University, Seoul, Korea, in 1983 and 1985, respectively, and the Dr. Eng. Degree from the University of Tokyo, Tokyo, Japan, in 1990. His doctoral dissertation concerned modeling, design, fabrication, and testing of microlinear actuators in magnetic levitation using high critical temperature superconductors. In 1990, he joined the Central Research Laboratory, Hitachi Ltd., Tokyo, Japan, where he was a Researcher involved with actuators of hard disk drives. In 1992, he joined the Seoul National University, where he is currently an Associate Professor of electrical engineering. His current research interests are modeling, design, and fabrication and testing of electric machines, especially MEMS, microsensors, and actuators.